

Article

Model-Free Adaptive Nonsingular Fast Integral Terminal Sliding Mode Control for Wastewater Treatment Plants

Baochang Xu , Zhongjun Wang, Zhongyao Liu, Yiqi Chen and Yaxin Wang

College of Information Science and Engineering, China University of Petroleum, Beijing 102249, China; wangzj_cup@163.com (Z.W.); liuzy_cup@163.com (Z.L.); chenyaqi_cup@163.com (Y.C.); wangyx_cup@163.com (Y.W.)

* Correspondence: xbcyl@cup.edu.cn

Abstract: The regulation of wastewater treatment plants (WWTPs) is a challenge due to their complex biological and chemical characteristics and their accurate mathematical model is generally not accessible because of the limitation of available measurements. To overcome such challenges, in this paper, a novel model-free adaptive nonsingular fast integral terminal sliding mode control (MFA-NFITSMC) is proposed. Firstly, based on the concept of dynamic linearization, a compact format dynamic linearized (CFDL) data model for the WWTP is established. Secondly, a novel fast integral terminal sliding mode surface is proposed to accelerate the convergence of tracking error and a discrete-time MFA-NFITSMC is created using the CFDL model as a basis; then, its stability is proved by theoretical analysis. Finally, the experimental verification is conducted based on the Benchmark Simulation Model No. 1 and the results show that the proposed method has a higher tracking accuracy and stronger robustness than other methods in the control of WWTPs.

Keywords: wastewater treatment; dissolved oxygen; data-driven control; model-free adaptive control; dynamic linearization; fast integral terminal sliding mode control



Citation: Xu, B.; Wang, Z.; Liu, Z.; Chen, Y.; Wang, Y. Model-Free Adaptive Nonsingular Fast Integral Terminal Sliding Mode Control for Wastewater Treatment Plants. *Appl. Sci.* **2023**, *13*, 13023. <https://doi.org/10.3390/app132413023>

Academic Editor: Dino Musmarra

Received: 1 November 2023

Revised: 17 November 2023

Accepted: 30 November 2023

Published: 6 December 2023



Copyright: © 2023 by the authors. Licensee MDPI, Basel, Switzerland. This article is an open access article distributed under the terms and conditions of the Creative Commons Attribution (CC BY) license (<https://creativecommons.org/licenses/by/4.0/>).

1. Introduction

With the rapid development of the economy and the advancement of urban industrialization, the discharge of industrial wastewater and domestic wastewater is becoming increasingly severe. The contradiction between the supply and demand of water has been severely exacerbated by the shortage of available water caused by water pollution and the increasing water demand and has become a common problem facing the world. Wastewater treatment plants (WWTPs) are industrial systems widely used in petrochemical and residential life fields. They can reduce water pollution, promote wastewater recycling, greatly reduce industrial water demand, and avoid environmental pollution. However, WWTPs are very complex time-varying dynamic systems and their internal reaction processes are influenced by the influent flow rate, pollutant load, and unknown inflow components, exhibiting characteristics such as nonlinearity, strong coupling, and strong disturbance [1]. Therefore, research on the control of wastewater treatment plants is of great significance for improving operational performance and improving effluent quality.

To meet the treatment efficiency standards of WWTPs, there have been many groundbreaking research developments in recent years. Traditional control strategies such as on-off switch control, PID control, PI feedforward control, and their combination forms have been widely employed to regulate the concentrations of nitrate nitrogen and dissolved oxygen (DO) [2,3]. However, due to the inability of the above controller parameters to adaptively change online, the control performance of the WWTP system will be affected when it is subjected to external disturbances such as influent flow. In response to this problem, a fuzzy control algorithm [4] is proposed to control the DO concentration. Compared with traditional switch control laws, the control deviation is improved by 60% and

the energy consumption is reduced by more than 40%. Since then, more and more fuzzy control strategies [5,6] have been applied to WWTPs, which have greatly improved control effectiveness and reduced energy consumption. Nevertheless, these tactics are challenging to implement in real life and mostly rely on the experience of experts.

To improve the control accuracy, some model-based control algorithms have been applied to WWTPs, such as model predictive control (MPC) [7], adaptive control [8], and adaptive sliding-mode control [9]. Although it is challenging to create a precise mathematical model of a WWTP due to its strong nonlinear and non-stationary dynamic properties, model-based control strategies frequently use a linearization method near the operating point, using a reduced-order model to approximate the actual model. This will cause some dynamic characteristics of the high-order system to be neglected, leading to unmodeled dynamic problems. Therefore, it is challenging to obtain satisfactory results using model-based control systems in industrial practice. To address the above issues, neural networks have been applied to the identification and control of unknown dynamic systems in WWTPs. Qiao et al. [10] proposed a multivariable PI control algorithm based on a feedforward neural network model and an adaptive fuzzy neural network control algorithm [11]. Han et al. [12–15] proposed nonlinear model predictive control strategies for WWTPs which have shown good performance in robustness and energy conservation. However, control strategies based on neural networks require a large amount of historical data for training and, for most WWTPs, due to limitations in measurement equipment, it is not possible to provide a large amount of data that can be used to train models. In a broad sense, a neural network is the model of a system. When the system changes, the network needs to be retrained and the determination of network nodes and hidden layers requires prior knowledge of the controlled object. Therefore, control strategies based on neural networks still cannot avoid unmodeled dynamic problems.

Currently, data-driven techniques have been used in fields such as control, decision-making, scheduling, and fault diagnosis. Hou et al. [16,17] proposed a data-driven modeling technique for nonlinear systems called compact format dynamic linearization (CFDL). This method only relies on the input and output (I/O) data of the control system, does not need any system model, and implements model-free adaptive control (MFAC) for unknown control systems. Up to now, CFDL data-driven modeling methods have played an important role in many fields [18–20]. Through theoretical analysis, simulation research, and practical applications, it has been demonstrated that the data-driven CFDL modeling method produced a control system with strong robustness, simplicity, practicality, low computational complexity, and ease of implementation. Unmodeled dynamical problems of unknown nonlinear time-varying systems can be effectively solved with this technique [16,17]. Meanwhile, sliding mode control (SMC) can force the current state of the system (such as errors and their derivatives) to move according to the predetermined sliding mode state trajectory during dynamic processes. Due to the design of the sliding surface being independent of target parameters and disturbances, SMC has the advantages of fast response, insensitivity to parameter changes and disturbances, and simple physical implementation. Understanding the control system's mathematical model is necessary for designing SMC controllers. Therefore, designing SMC based on CFDL data models is of great significance for simultaneously leveraging their advantages [21–23].

Motivated by the above discussion and aiming at the characteristics of the WWTP, such as the difficulty of accurate modeling and the existence of unknown interference, this paper establishes a CFDL data model for the WWTP and proposes a data-driven model-free adaptive nonsingular fast integral terminal sliding mode control (MFA-NFITSMC) strategy. The advantages of this strategy are as follows:

- (1) The proposed method does not rely on the mathematical model or human experience of WWTP and only requires real-time I/O measurement data. It can effectively avoid the uncertainty of the model and the impact of unmodeled dynamics on the closed-loop system.

- (2) A novel fast integral terminal sliding mode surface (FITSMS) is proposed to ensure that the tracking error can converge quickly when it is far from the equilibrium point. This addresses the issue that the conventional integral sliding mode control (ISMC) cannot ensure that the system state converges to zero in a finite time and the rate of convergence of the tracking error is slow.
- (3) The BSM was used to validate the suggested approach’s control performance and it was contrasted with other control schemes including PID and MPC. The simulation experiment results indicate that the MFA-NFITSMC strategy has a better tracking performance and stronger robustness in the control of WWTP.

2. Problem Description

In this section, the layout and dynamic model of the BSM1 will be introduced and a CFDL data model for WWTP based on dynamic linearization technology will be established.

2.1. Benchmark Simulation Model No. 1 (BSM1)

To effectively evaluate wastewater treatment control strategies, the European Cooperation in Science and Technology (COST) and the International Water Association (IWA) jointly developed the benchmark simulation model BSM1 for the activated sludge method [24]. Figure 1 shows the general layout of the model’s two components, the biochemical reactor and the secondary clarifier. The biochemical reactor consists of two anoxic tanks and three aerobic tanks. The activated sludge model No. 1 (ASM1), which has 13 components in Table 1, 8 biochemical reaction processes, and 19 parameters, was adopted by the mechanistic model of the biochemical reaction. The secondary clarifier, which has 10 layers, is where the wastewater goes after the biochemical reaction. The primary purpose of the secondary clarifier is to use sedimentation to separate mud and water. After sedimentation, the upper layer of clear water is discharged and the lower layer of sludge is sent in two parts—partly to the biochemical reaction to take part in the reaction and partly to be drained from the system. The secondary clarifier’s mechanism model uses a double-exponential sedimentation velocity model.

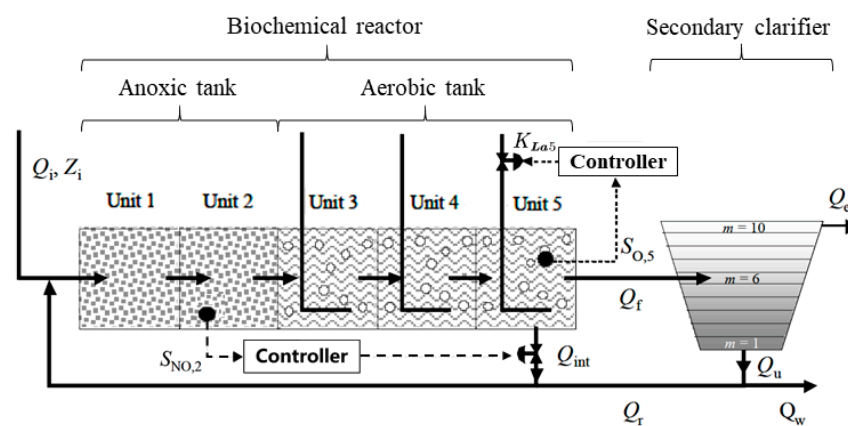


Figure 1. The process flow diagram of BSM1.

Due to the significant biochemical reactions and main operating variable quantity of WWTPs occurring in ASM1, a large amount of research has focused on this. The general formula for mass conservation in ASM1 can be expressed as follows:

$$\frac{dZ_k}{dt} = \begin{cases} \frac{Q_{int}Z_{int} + Q_r Z_r + Q_i Z_i + r_1 V_1 - Q_1 Z_1}{V_1}, k = 1 \\ \frac{Q_{k-1} Z_{k-1} + r_k V_k - Q_k Z_k}{V_k}, k = 2 \sim 5 \end{cases} \quad (1)$$

where V_k represents the volume of unit k , and r_k , Q_k , and Z_k respectively represent the reaction rate, flow rate, and concentration of each component in unit k . Similarly, subscripts r , int , and i represent external reflux, internal reflux, and inflow, respectively.

Table 1. List of ASM1 variables.

Notation	Definition
S_I	Soluble inert organic matter
S_S	Readily biodegradable substrate
X_I	Particulate inert organic matter
X_S	Slowly biodegradable substrate
$X_{B,H}$	Active heterotrophic biomass
$X_{B,A}$	Active autotrophic biomass
X_P	Particulate products arising from biomass decay
S_O	Oxygen
S_{NO}	Nitrate and nitrite nitrogen
S_{NH}	NH_4^+ + NH_3 nitrogen
S_{ND}	Soluble biodegradable organic nitrogen
X_{ND}	Particulate biodegradable organic nitrogen
S_{ALK}	Alkalinity

Studies reveal that the nitrate concentration in unit 2 ($S_{NO,2}$) and the DO concentration in unit 5 ($S_{O,5}$) are directly related to the quality of effluent and they are essential to the effectiveness of wastewater treatment. In BSM1, the control of $S_{NO,2}$ and $S_{O,5}$ is achieved by controlling the internal return flow rate (Q_{int}) and the oxygen transfer coefficient (K_{La5}) of unit 5. The variation of $S_{NO,2}$ can be represented by Equation (1) and the variation of $S_{O,5}$ can be expressed as:

$$\frac{dS_{O,5}}{dt} = \frac{1}{V_5} (Q_4 S_{O,4} + r_5 V_5 - Q_5 S_{O,5} + (K_{La5}) V_5 (S_{O,sat} - S_{O,5})) \tag{2}$$

where $S_{O,sat}$ is the DO saturation concentration, which is usually taken as 8 g/m³.

2.2. CFDL Model for WWTP

Taking the DO concentration as an example, the nonlinear discrete system of the $S_{O,5}$ in a WWTP can be expressed as:

$$y(k + 1) = f(y(k), y(k - 1), \dots, y(k - n_y), u(k), u(k - 1), \dots, u(k - n_u)) \tag{3}$$

where $u(k) \in R$ represents the system input K_{La5} , $y(k) \in R$ indicates the system output $S_{O,5}$, n_u and n_y indicate the input and output order of the system, and $f(\cdot)$ represents a nonlinear function which is unknown.

Based on the CFDL theory [25], reasonable assumptions are introduced for the WWTP system shown in Equation (2).

Assumption 1. The partial derivative of $f(\cdot)$ in (3) is continuous under the action of the control input K_{La5} .

Assumption 2. The generalized Lipschitz condition is met by the WWTP system (3) that is, at any particular moment k , if $\Delta u(k) \neq 0$, then $|y(k + 1) - y(k)| \leq b|\Delta u(k)|$, where the constant b is positive.

Remark 1. Indeed, the input-output change rate of a nonlinear control system for a WWTP is typically constrained by Assumption 1. A bounded input energy change should result in a bounded output energy change inside the system, since the WWTP complies with the rule of energy conservation, satisfying Assumptions 1 and 2.

For a WWTP system satisfying the above assumptions, we have Lemma 1 as follows.

Lemma 1. For the system (3) of $S_{O,5}$ in a WWTP satisfying Assumptions 1 and 2, when $|\Delta u(k)| \neq 0$ at time k , there is a time-varying parameter $\phi_c(k) \in R$ referred to as the pseudo partial derivative (PPD), that system (2) can be converted into the following model:

$$\Delta y(k + 1) = \phi_c(k)\Delta u(k) \tag{4}$$

where $\phi_c(k)$ is bounded for any time k .

For the unknown PPD $\phi_c(k)$ in the data model (4) with dynamic linearized, an improved projection algorithm is used for estimation, considering the following PPD estimation criterion function:

$$J(\phi_c(k)) = |y(k) - y(k - 1) - \phi_c(k)\Delta u(k - 1)|^2 + \mu|\phi_c(k) - \hat{\phi}_c(k - 1)|^2 \tag{5}$$

where $\mu > 0$ is the weighting factor.

Let $\partial J/\partial \phi_c(k) = 0$, then the estimation formula of $\phi_c(k)$ can be computed in the following way:

$$\hat{\phi}_c(k) = \hat{\phi}_c(k - 1) + \frac{\eta \Delta u(k - 1)(\Delta y(k) - \hat{\phi}_c(k - 1)\Delta u(k - 1))}{\mu + \Delta u(k - 1)^2} \tag{6}$$

where $\eta \in (0, 1]$ denotes the weighting factor, which is aimed to make the algorithm more flexible and general. $\hat{\phi}_c(k)$ represents the estimation of $\phi_c(k)$.

Due to the fact that the WWTP is a typical time-varying system with significant parameters change, in order to enhance the tracking ability of PPD estimation algorithm (6) for time-varying parameters, when $|\hat{\phi}_c(k)| \leq \varepsilon$ or $|\Delta u(k - 1)| \leq \varepsilon$, make

$$\hat{\phi}_c(k) = \hat{\phi}_c(1) \tag{7}$$

where ε is a sufficiently small positive number usually taken as 10^{-5} , and $\hat{\phi}_c(1)$ is the initial value of $\hat{\phi}_c(k)$. Combining Equations (4), (6) and (7) can obtain the CFDL data model for the WWTP:

$$y(k + 1) = y(k) + \hat{\phi}_c(k)\Delta u(k) \tag{8}$$

3. Controller Design for WWTP

In this section, a fast integral terminal sliding mode surface is proposed and a discrete time model-free adaptive nonsingular fast integral terminal sliding mode controller is designed based on the dynamic linearization data model of WWTP. The stability of the closed-loop system is demonstrated through theoretical analysis.

3.1. Fast Integral Terminal Sliding Mode Surface

There are two phases to the SMC design. Creating the sliding mode surface is the first step in forcing the system state to reach the equilibrium point. Creating the reaching law is the second step in making sure the system's motion trajectory is driven to and maintained on the sliding mode surface. The robustness of the system during the arrival stage cannot be guaranteed by a standard SMC. To solve this problem, integral sliding mode control (ISMC) is introduced to eliminate the reaching phase.

Describing the tracking error of the system $e = y_d - y$, where y_d is the desired output, y is the system output, then ISMC's sliding mode surface is created as:

$$s(t) = e(t) + k \int_0^t e(\tau) d\tau \tag{9}$$

where $k > 0$ is a coefficient that requires designing.

Assuming the initial tracking error is $e(0)$, when the integral in Equation (9) has the initial value $-e(0)/k$, $s(t)$ starts at zero and stays there for the duration of the system response. On the manifold $s(t) = 0$ of ISMC, we have

$$e(t) = e(0) \exp(-kt) \tag{10}$$

which suggests that there is no guarantee that the tracking error will converge to zero in a finite amount of time. To solve this problem, the ISMC is combined with the terminal sliding mode control (TSMC) which makes finite-time tracking possible. The sliding mode surface of the integral terminal sliding mode control (ITSMC) is intended to be:

$$s(t) = e(t) + \alpha \int_0^t e^{p_1/p_2}(\tau) d\tau \tag{11}$$

where $\alpha > 0$ is a coefficient that requires designing, p_1 and p_2 are positive odd integers satisfying $p_2 > p_1 > 0$.

For Equation (11), define the integral term $e_I(t) = \int_0^t e^{p_1/p_2}(\tau) d\tau$, and ensure $e_I(0) = -e(0)/\alpha$, when $s(t) = 0$ (i.e., $e(t) = -\alpha e_I(t)$), we have

$$\dot{e}_I(t) = -\alpha^{p_1/p_2} e_I^{p_1/p_2}(t) \tag{12}$$

The convergent time of $e_I(t)$ can be obtained by solving the error dynamic Equation (12) as follows:

$$T_{f1} = \frac{|e_I(0)|^{1-p_1/p_2}}{\alpha^{p_1/p_2}(1-p_1/p_2)} = \frac{|e(0)|^{1-p_1/p_2}}{\alpha(1-p_1/p_2)} \tag{13}$$

which indicates that in a limited amount of time T_{f1} , the tracking error, can converge to zero.

Since $p_1/p_2 < 1$, when far away from the equilibrium point, i.e., $|e_I(t)| \gg 1$, the value of $|\dot{e}_I(t)|$ will significantly decrease according to Equation (12); thus, the convergence speed of $e_I(t)$ will be greatly reduced. To solve this problem, according to the research of Chiu [26], a FITSMS with fast convergence properties is intended to be:

$$s(t) = e(t) + \int_0^t [\alpha |e(\tau)|^{p_1/p_2} \text{sgn}(e(\tau)) + \beta \text{sgn}(e(\tau))] d\tau \tag{14}$$

where $e(t)$, α , p_1 , and p_2 have the same definition as in Equation (11), and $\beta > 0$ is a coefficient that requires designing. The difference between the fractional order term in the integral term and Equation (11) is to ensure that when the error is negative, the calculation result is a real number. It is essentially the same as Equation (11).

Theorem 1. For the WWTP system shown in Equation (8), using FITSMS based on Equation (14), when the tracking error is on the sliding mode surface, the tracking error can converge to zero in a finite time to make the WWTP system stable.

Proof of Theorem 1. Assuming only the second term of the integral term in Equation (14) is considered, we have

$$s(t) = e(t) + \int_0^t \beta \text{sgn}(e(\tau)) d\tau \tag{15}$$

For Equation (15), define the integral term $e_I(t) = \int_0^t \beta \text{sgn}(e(\tau)) d\tau$, and ensure $e_I(0) = -e(0)/\beta$, when $s(t) = 0$ (i.e., $e(t) = -\beta e_I(t)$), we have

$$\dot{e}_I(t) = -\text{sign}(\alpha e_I(t)) \tag{16}$$

The convergent time of $e_I(t)$ can be found by solving the error dynamic Equation (16) as follows:

$$T_{f2} = |e_I(0)| = \frac{e(0)}{\beta} \tag{17}$$

By combining Equation (13), the convergence time of FITSMS can be obtained

$$T_f < \min\left(\frac{|e(0)|^{1-p_1/p_2}}{\alpha(1-p_1/p_2)}, \frac{|e(0)|}{\beta}\right) \tag{18}$$

Due to the initial the tracking error $e(0)$ of the DO concentration is bounded and non-zero, the convergence time T_f is also bounded. Therefore, the tracking error of the DO concentration satisfies the finite time convergence on the FITSMS, and

$$T_f < T_{f1} \tag{19}$$

The convergence time T_f can be adjusted by adjusting α and β . Thus, Theorem 1 is proved. \square

Compared with Equation (9), Equation (12) contains an integral term of $\beta \text{sign}(e)$, so when the system state is far from the equilibrium point, the tracking error converges faster. In fact, due to the effect of the integral sliding mode term, the integral term's starting value $-e(0)$ guarantees that $s(t)$ stays at zero at all times, thereby ensure the global robustness of the system.

3.2. MFA-NFITSMC Design

For the system shown in Equation (8), the discrete time tracking error is defined as follows:

$$e(k) = y_d(k) - y(k) \tag{20}$$

where $y_d(k)$ is the desired output at time k , $y(k)$ is the system output at time k .

The discrete form of the FITSMS (12) is defined as follows:

$$s(k) = e(k) + TE(k - 1) \tag{21}$$

where T is the sample time. The integral error term is

$$\begin{aligned} E(k) &= \sum_{i=1}^k \left[\alpha |e(i)|^{\frac{p_1}{p_2}} \text{sgn}(e(i)) + \beta \text{sgn}(e(i)) \right] \\ &= E(k - 1) + \alpha |e(k)|^{p_1/p_2} \text{sgn}(e(k)) + \beta \text{sgn}(e(k)) \end{aligned} \tag{22}$$

Due to the interference of the inlet flow rate and the unknown component concentration in WWTP, the tracking error of the DO concentration cannot always be on the sliding surface, which will lead to a deterioration of the global robustness of the system. In order to meet the reachability of tracking error to sliding mode surface, accelerate convergence speed, and reduce chattering, the following approach law [27] is selected:

$$\dot{s} = -m|s|^\lambda \text{sgn}(s) - ns \tag{23}$$

where m and n are constants that are positive, $0 < \lambda < 1$. Its discrete form is as follows:

$$s(k + 1) - s(k) = -mT|s(k)|^\lambda \text{sgn}(s(k)) - nTs(k) \tag{24}$$

Considering Equations (8) and (20)–(22), we can obtain

$$\begin{aligned}
 s(k+1) - s(k) &= e(k+1) + TE(k) - e(k) - TE(k-1) \\
 &= y_d(k+1) - y(k+1) - (y_d(k) - y(k)) + T \left(\alpha |e(k)|^{\frac{p_1}{p_2}} \text{sgn}(e(k)) + \beta \text{sgn}(e(k)) \right) \quad (25) \\
 &= \Delta y_d(k) - \hat{\phi}_c(k) \Delta u(k) + T \left(\alpha |e(k)|^{p_1/p_2} \text{sgn}(e(k)) + \beta \text{sgn}(e(k)) \right)
 \end{aligned}$$

By combining Equations (24) and (25), the following control law can be obtained

$$\Delta u(k) = \frac{1}{\hat{\phi}_c(k)} (mT|s(k)|^\lambda \text{sgn}(s(k)) + nTs(k) + \Delta y_d(k) + \alpha T|e(k)|^{p_1/p_2} \text{sgn}(e(k)) + \beta T \text{sgn}(e(k))) \quad (26)$$

In Equation (26), the desired output increment $\Delta y_d(k)$ is required to calculate the control variable. In fact, the trajectory to be tracked is usually predefined in the control system, so $\Delta y_d(k)$ is a priori known. When the desired output is a constant value, Equation (26) can be expressed as:

$$\Delta u(k) = \frac{1}{\hat{\phi}_c(k)} (mT|s(k)|^\lambda \text{sgn}(s(k)) + nTs(k) + \alpha T|e(k)|^{\frac{p_1}{p_2}} \text{sgn}(e(k)) + \beta T \text{sgn}(e(k))) \quad (27)$$

Hou and Jin [25] have proved that the PPD estimation value $\hat{\phi}_c(k)$ is bounded and the reset algorithm (7) guarantees that the lower bound of $\hat{\phi}_c(k)$ is not zero, so the control law given by Equation (27) is nonsingular. Thus, a complete MFA-NFITSMC method for the WWTP control system is constructed by Equations (4)–(7) and (20)–(27), and the structure of control system is shown in Figure 2.

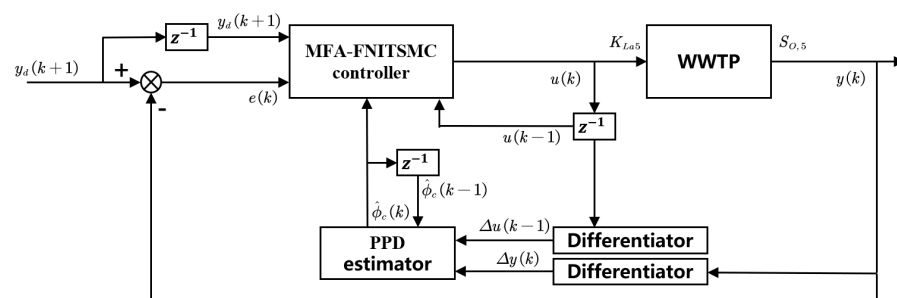


Figure 2. The control flow chart.

3.3. Stability Analysis

To demonstrate the stability of the designed WWTP control system, the following assumptions are added:

Assumption 3. Every time a bounded expected output signal $y_d(k+1)$ is given, a bounded $u(k)$ always exists, so that the system's output approach is $y_d(k+1)$ driven by this control input signal.

Assumption 4. At any time k , when $\Delta u(k) \neq 0$, the sign of the system's PPD remains unchanged; that is, $\phi_c(k) > \epsilon > 0$ or $\phi_c(k) < -\epsilon$, where ϵ is a small positive constant.

Remark 2. Assumption 3 is a necessary condition for system controllability. Assumption 4 suggests that the system output should not decrease in proportion to an increase in the control input, which can be considered as a quasi-linear characteristic of the system. Obviously, the WWTP system meets the above assumptions.

Theorem 2. For the WWTP system in Equation (3), under the conditions of Assumptions 1–4, when $y_d(k+1) = y_d = \text{const}$, using the MFA-NFITSMC control strategy in Equation (27), there are:

- (1) The WWTP system's tracking error is convergent., and $\lim_{k \rightarrow \infty} |y_d(k+1) - y(k+1)| = 0$.
- (2) The output and input sequences $\{y(k)\}$ and $\{u(k)\}$ are bounded.

Proof of Theorem 2. The following one-step forward sliding mode function can be obtained from Equation (21):

$$s(k + 1) = e(k + 1) + TE(k) \tag{28}$$

By introducing Equation (20) into Equation (28) and considering Equations (8) and (25), it can be concluded that:

$$\begin{aligned} s(k + 1) &= y_d(k + 1) - y(k + 1) + TE(k) \\ &= y_d(k + 1) - (y(k) + \hat{\phi}_c(k)\Delta u(k)) + TE(k) \\ &= y_d(k + 1) - (y(k) + mT|s(k)|^\lambda \text{sgn}(s(k)) + nTs(k) \\ &\quad + \alpha T|e(k)|^{\frac{p_1}{p_2}} \text{sgn}(e(k)) + \beta T \text{sgn}(e(k))) + TE(k) \\ &= e(k) + TE(k - 1) - mT|s(k)|^\lambda \text{sgn}(s(k)) - nTs(k) \\ &= s(k) - mT|s(k)|^\lambda \text{sgn}(s(k)) - nTs(k) \end{aligned} \tag{29}$$

Thus

$$s(k + 1) - s(k) = -mT|s(k)|^\lambda \text{sgn}(s(k)) - nTs(k) \tag{30}$$

Since both m and n are greater than 0, when $s(k) > 0$

$$s(k + 1) - s(k) < 0 \tag{31}$$

and when $s(k) < 0$

$$s(k + 1) - s(k) > 0 \tag{32}$$

Considering Equations (31) and (32), it can be concluded that

$$s(k + 1) < s(k), s(k) > 0 \quad s(k + 1) > s(k), s(k) < 0 \tag{33}$$

Equation (33) satisfies the existence and arrival conditions of a discrete sliding mode

$$[s(k + 1) - s(k)]\text{sgn}(s(k)) < 0 \quad [s(k + 1) + s(k)]\text{sgn}(s(k)) > 0 \tag{34}$$

Therefore, $s(k)$ is monotonically decreasing and Equation (34) is a necessary and sufficient condition for the existence of discrete quasi sliding mode states [28]. This means that under the action of Equation (27), the tracking error of the WWTP system can converge to the neighborhood of zero, that is, $\{e(k)\}$ is bounded. According to Theorem 1, $e(k)$ can converge to zero in a finite time, i.e., $\lim_{k \rightarrow \infty} |y_d(k + 1) - y(k + 1)| = 0$.

The tracking error is defined as $e(k) = y_d(k) - y(k)$; given that $\{y_d(k)\}$ is bounded and it has been proven that $\{e(k)\}$ is bounded, thus $\{y(k)\}$ is bounded. According to the zero dynamic characteristics of the system's asymptotic stability, there are constants a, b , and k_0 that satisfy:

$$|\Delta u(k - 1)| \leq |a \max_{\tau < k} |y(\tau)| + b, \forall k > k_0 \tag{35}$$

That is, $\{u(k)\}$ is bounded. Thus, Theorem 2 is proved. \square

Remark 3. The $\beta \text{sgn}(e(k))$ in Equation (27) will cause higher chattering, the sign function is replaced with the sigmoid function, which is given below, in order to lessen the chattering it causes.

$$\text{sigmoid}(\sigma, e(k)) = \frac{2}{1 + \exp(-\sigma e(k))} - 1 \tag{36}$$

where $\sigma > 0$ and $\sigma = 2$ is chosen in order to obtain a balance between chattering and robustness.

4. Simulation

In Figure 1, the BSM1 employs the constructed MFA-NFITSMC to confirm the intended method’s control effect. The BSM1 used the rainy and dry weather input data files, which came from the working groups of COST Actions 682 and 624. These files were downloaded as normative data to be used in the controller evaluation. Figure 3 shows the dynamic inflow data and key component concentrations on dry and rainy weather from the 7th day to the 14th day, including the influent flow Q_i , the ammonia nitrogen S_{NH} , and the readily biodegradable substrate S_S . The operating period is two weeks, with a sampling interval of 15 min. The inflow data from the previous week is used to stabilize the system, while the dynamic data from the following week is used to test the controller performance. The MFA-NFITSMC parameters are set as follows: $T = 10^{-5}$ day, $m = 0.1$, $n = 0.1$, $\alpha = 10$, $\beta = 15$, $q_1 = 3$, $q_2 = 5$, $\lambda = 0.6$, $\phi_c(0) = 0.2$, $\eta = 0.8$, $\mu = 1$. For model-free adaptive integral terminal sliding mode control (MFA-ITSMC), simply set $\beta = 0$, and the other parameters are the same as above. Furthermore, $u_{min} = 0$ and $u_{max} = 360$ are assigned to the actuator constraints’ upper and lower bounds, respectively. The evaluation of the system control effectiveness is mainly based on the following indicators

$$\begin{cases} ISE = \int_{t_0}^{t_f} e_i^2 dt \\ IAE = \int_{t_0}^{t_f} |e_i| dt \\ Dev_{max} = \max|e_i| \end{cases} \quad (37)$$

where the control system’s response rate is indicated by the integral of square error (ISE), the transient response and appropriate damping are indicated by the integral of absolute error (IAE), and the stability of the control system is indicated by the maximal absolute deviation (Dev_{max}), respectively.

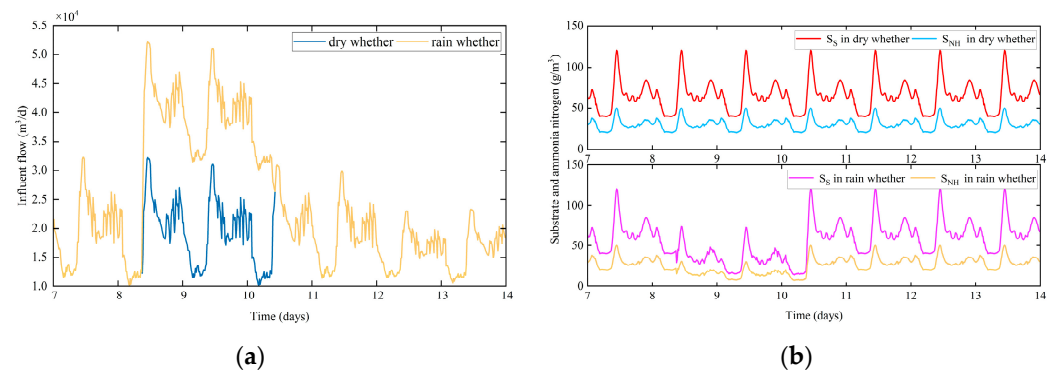


Figure 3. Dry and rainy weather influent. (a) Flow rate Q_i ; (b) Constituent concentrations S_S and S_{NH} .

Case 1. Usually, when the fifth unit’s DO concentration is maintained around 2 mg/L, the effluent quality meets the standard. Therefore, there are two types of reference trajectories in Case 1. $S_{O5ref} = 2$ mg/L is the first time-invariant reference trajectory of DO. The second is the DO reference trajectory S_{O5ref} that varies over time and includes 2 mg/L from days 7–9, 1.9 mg/L from days 9–11, 2.2 mg/L from days 11–12 and 2 mg/L from days 12–14. Considering the external interference of influent flow and component concentration in Figure 3, the controller performance was tested on dry and rainy weather and compared with other methods.

The proposed method’s control effect on the DO concentration in the WWTP is shown in Figures 4 and 5. The results show that the MFA-NFITSMC strategy can ensure the tracking of the DO concentration to the reference value under different weather conditions and reference trajectory; it has a fast response speed and strong anti-interference ability, and the control effect is better than PID and MFA-ITSMC methods. Tables 2 and 3 show the control effects of different control strategies on DO concentration on dry and rainy

weather using three evaluation indicators: ISE , IAE , and Dev_{max} . It can be seen that MFA-NFITSMC is better than other control strategies for all indicators. Therefore, the proposed method has a better tracking performance and is suitable for a WWTP with strong disturbances.

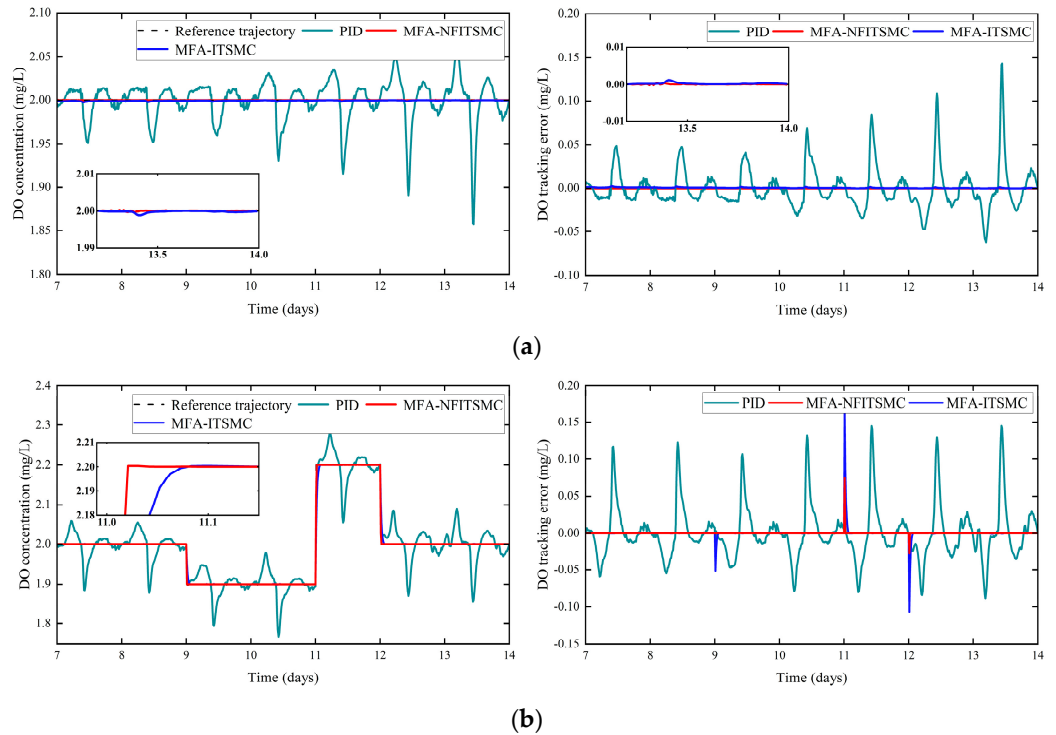


Figure 4. DO control effect under different controllers in dry weather. (a) DO tracking effect of trajectory 1 in dry weather; (b) DO tracking effect of trajectory 2 in dry weather.

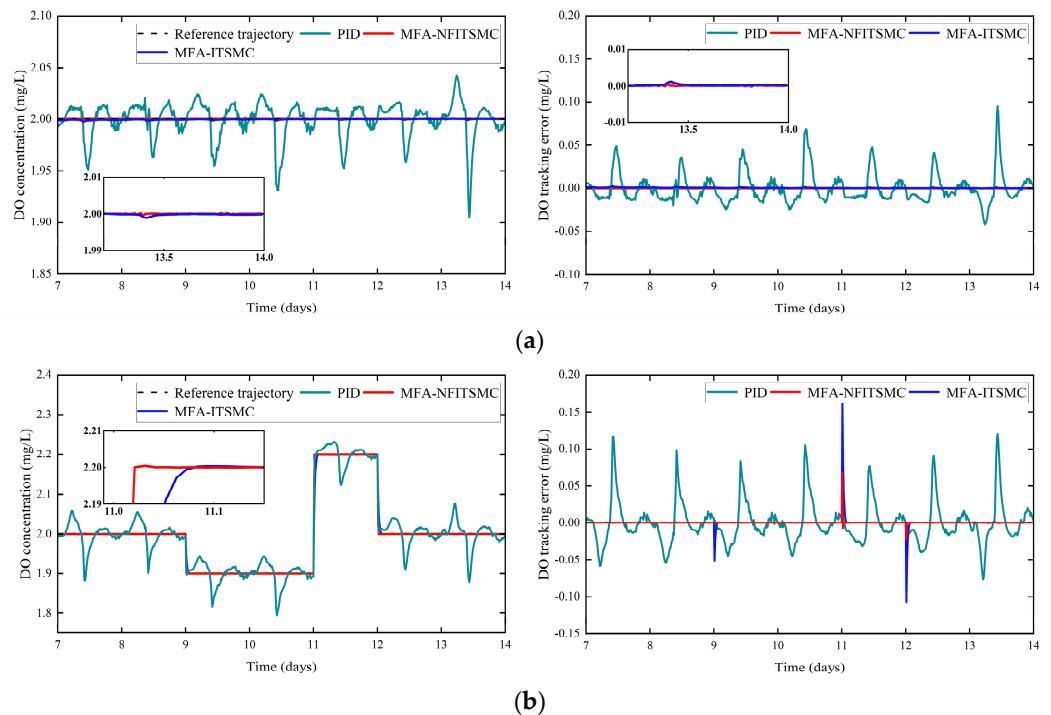


Figure 5. DO control effect under different controllers in rainy weather. (a) DO tracking effect of trajectory 1 in rainy weather; (b) DO tracking effect of trajectory 2 in rainy weather.

Table 2. The comparison of the performance of various control strategies for an invariant trajectory in Case 1’s dry weather.

Control Strategy	ISE	IAE	Dev _{max}
MFA-NFITSMC	0.00014	0.0273	0.0083
OS-ELM [29]	0.00069 *	0.0475 *	0.0381 *
PI + AT [30]	0.0009 *	0.0490 *	-
AFC [31]	0.0012 *	0.0792 *	0.0198 *
MPC [7]	0.0026 *	0.0890 *	0.0781 *
BFC [31]	0.0049 *	0.1507 *	0.0578 *
PID	0.0078	0.1576	0.1425

* The data originates from the corresponding articles.

Table 3. The comparison of the performance of various control strategies for an invariant trajectory in Case 1’s rain weather.

Control Strategy	ISE	IAE	Dev _{max}
MFA-NFITSMC	0.00014	0.0273	0.0083
OS-ELM [29]	0.00067 *	0.0375 *	0.0389 *
NNOMC [10]	0.00053 *	0.0390 *	-
SR-RBF [15]	-	0.0630 *	-
RBFNNPID [32]	0.0025 *	0.0947 *	0.0694 *
SORBF-MPC [12]	-	0.0810 *	-
PID	0.0045	0.1239	0.0952

* The data originates from the corresponding articles.

Case 2. The inflow data (6 January 2022 to 29 July 2022) of an actual WWTP shown in Figure 6 is used to test MFA-NFITSMC, indicating that the external disturbance to WWTP is random rather than periodic. The actual WWTP consists of three anoxic tanks and five aerobic tanks, with physical parameters of $45.35 \times 4.85 \times 5$ m. It has three aeration fans, each with a flow rate of $90 \text{ m}^3/\text{min}$, a lift of 5 m, and a power of 110 kW, and its maximum processing capacity is $12,000 \text{ m}^3/\text{day}$. In Case 2, there are three different kinds of reference trajectories. $S_{O5ref} = 2 \text{ mg/L}$ is the first time-invariant DO reference trajectory. The second is the time-varying DO reference trajectory S_{O5ref} , including 2 mg/L from day 0–1, 2.3 mg/L from day 1–1.5, and 1.8 mg/L from day 1.5–2. Figure 6b shows the changes in DO concentration for the third reference trajectory S_{O5ref} , which corresponds to the practical reference trajectory.

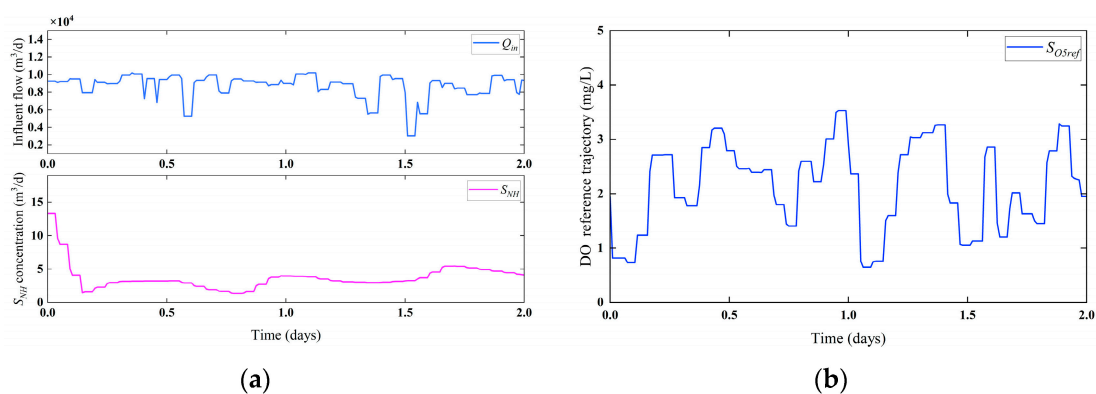


Figure 6. Influence information and trajectory changes in a real WWTP. (a) Flow rate and concentrations; (b) Practical reference trajectory changes.

Figure 7 shows the control effect of MFA-NFITSMC on DO concentration using actual data of a WWTP. The results show that the proposed method can effectively suppress nonperiodic disturbances in the WWTP system and has strong robustness. The three evaluation indicators of ISE, IAE, and Dev_{max} in Table 4 verify that the proposed method

has a good control performance, can accurately track time-varying reference trajectories, and has good dynamic performance.

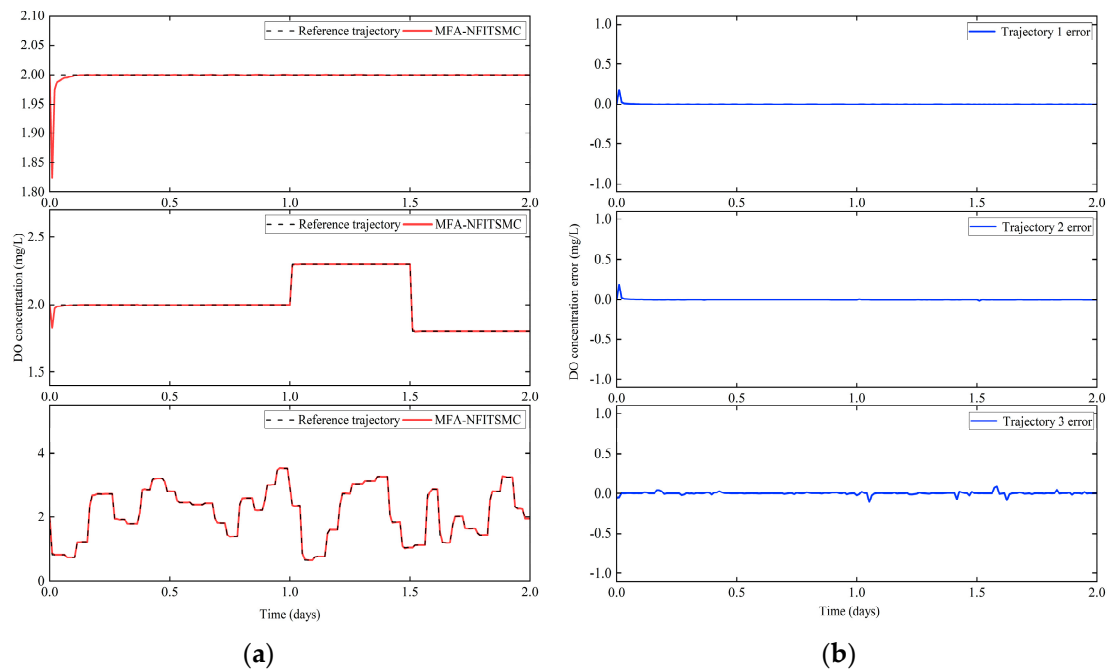


Figure 7. DO tracking effect using actual data. (a) DO control effect in Case 2; (b) DO tracking error in Case 2.

Table 4. Performance metrics of the proposed MFA-NFITSMC based on Case 2’s real data.

Reference Trajectory	ISE	IAE	Dev _{max}
Trajectory 1	3.3604×10^{-4}	0.0031	0.1768
Trajectory 2	3.4848×10^{-4}	0.0042	0.1768
Trajectory 3	5.2901×10^{-4}	0.0142	0.1004

Case 3. As key indicators in WWTP, S_{NO_2} and S_{O_5} need to be controlled within a reasonable range. However, controlling S_{NO_2} by adjusting the internal recycle flow rate can also cause significant interference with S_{O_5} . Traditional methods are difficult to effectively control S_{NO_2} and S_{O_5} simultaneously. To verify the control effect of the proposed method, two independent MFA-NFITSMC controllers are used to control the second unit nitrate nitrogen concentration and the fifth unit DO concentration in rainy whether. The reference trajectory of nitrate nitrogen concentration is set to $S_{NO_2ref} = 1 \text{ mg/L}$ and the reference trajectory of DO concentration is set to $S_{O_5ref} = 2 \text{ mg/L}$. The controller parameters for nitrate nitrogen are set to: $m = 0.5$, $n = 0.5$, $\alpha = 20$, $\beta = 30$, $\phi_c(0) = 0.0001$; other parameters are the same as the DO controller. Furthermore, $u_{min} = 0$ and $u_{max} = 92,230$ are assigned to the lower and upper bounds of the actuator constraints, respectively.

The control effect of the proposed method on the DO concentration and the nitrate nitrogen concentration in the WWTP is shown in Figure 8. The outcomes demonstrate MFA-NFITSMC’s good performance in the control of S_{NO_2} and S_{O_5} , with a control error of $\pm 0.05 \text{ mg/L}$ for S_{NO_2} and $\pm 0.015 \text{ mg/L}$ for S_{O_5} . Table 5 compares the three evaluation indicators of ISE, IAE, and Dev_{max} with PID, SMC, and ASMC strategies. The results show that the MFA-NFITSMC strategy is better than other strategies in all indicators, with higher control accuracy and stronger robustness, and can effectively suppress internal and external disturbances in the WWTP system.

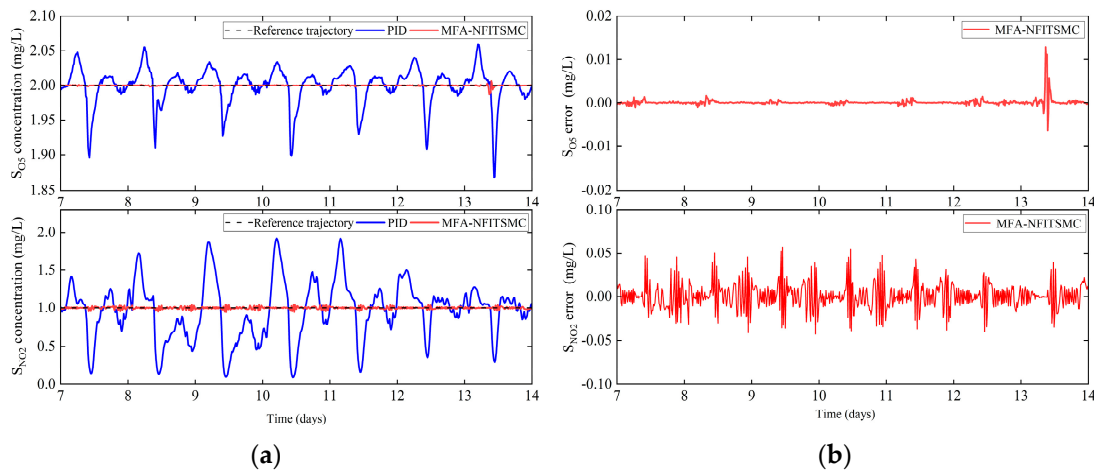


Figure 8. S_{O_5} and S_{NO_2} tracking effect in rainy weather. (a) Control effect of S_{O_5} and S_{NO_2} ; (b) Tracking error of S_{O_5} and S_{NO_2} .

Table 5. The comparison of the performance of different control algorithms in Case 3.

Control Strategy	S_{O_5}			S_{NO_2}		
	ISE	IAE	Dev _{max}	ISE	IAE	Dev _{max}
MFA-NFITSMC	0.00058	0.0013	0.0128	0.0016	0.0782	0.0571
ASMC [9]	0.00493 *	0.035 *	0.49 *	0.00527 *	0.046 *	0.42 *
SMC [9]	0.00552 *	0.030 *	0.61 *	0.00562 *	0.046 *	0.44 *
PID	0.0143	0.072	0.74	0.0081	0.056	0.53

* The data originates from the corresponding articles.

In summary, the proposed method can effectively control the WWTP system with nonlinear, slow time-varying, and strong disturbance characteristics. Compared with other methods, the MFA-NFITSMC method has a superior dynamic and steady-state performance and stronger robustness.

5. Conclusions

In this paper, a novel data-driven model-free adaptive nonsingular fast integral terminal sliding mode control algorithm is proposed to solve the problems of difficult to establish an accurate model and unknown disturbance in a WWTP. The proposed method doesn't need a precise mathematical model and prior knowledge of WWTP, only real-time I/O data, and has fast error convergence, nonsingular control law, and global robustness. Furthermore, the error convergence and BIBO stability of the closed-loop system have been proven through theoretical analysis. The simulation results in three cases indicate that compared with other control strategies, the MFA-NFITSMC has a higher control accuracy and stronger robustness in the control of WWTP and can effectively suppress the impact of unknown interferences on the WWTP system. In addition, the proposed method provides a new solution for the tracking control problem of a class of nonlinear slow time-varying and difficult to establish models for complex systems under multiple operating conditions.

Although the proposed method MFA-NFITSMC has achieved excellent results for the control of WWTPs, there are still some problems that need to be addressed urgently. For example, the selection of controller parameters was only obtained through a large number of experiments and further research work is focused on optimizing controller parameters and designing controllers for MIMO systems.

Author Contributions: Conceptualization, Supervision, B.X.; Methodology, Writing—original draft, Z.W.; Project administration, Z.L.; Writing—Review & Editing, Y.W.; Software, Validation, Y.C. All authors have read and agreed to the published version of the manuscript.

Funding: This research was funded by Research on the National Key Research and Development Program of China, Grant Number: 2019YFA0708304 and the Strategic Cooperation Technology Projects of CNPC and CUPB, Grant Number: ZLZX2020-03 and the National Natural Science Foundation of China, Grant Number: 52374015.

Data Availability Statement: The data presented in this study are available on request from the corresponding author. The data are not publicly available due to privacy.

Acknowledgments: Acknowledgements to Liuqiang Yue for providing funding acquisition, data calculation, and contributions during the article revision process. Acknowledgements to Qingsong Yang for providing funding for this project. Acknowledgements to Qin Yang for providing data support for this project. Acknowledgements to Xiaopeng Ma for analyzing on-site data. Acknowledgements to Li Hao for investigating the data required in the experiment.

Conflicts of Interest: The authors declare no conflict of interest.

References

1. *The Cost Simulation Benchmark-Description and Simulator Manual*; Office for Publications of the European Community: Luxembourg, 2001.
2. Suescun, J.; Irizar, I.; Ostolaza, X.; Ayesa, E. Dissolved oxygen control and simultaneous estimation of oxygen uptake rate in activated-sludge plants. *Water Environ. Res.* **1998**, *70*, 316–322. [[CrossRef](#)]
3. Wahab, N.A.; Katebi, R.; Balderud, J. Multivariable PID control design for activated sludge process with nitrification and denitrification. *Biochem. Eng. J.* **2009**, *45*, 239–248. [[CrossRef](#)]
4. Ferrer, J.; Rodrigo, M.A.; Seco, A.; Peña-Roja, J.M. Energy saving in the aeration process by fuzzy logic control. *Water Sci. Technol.* **1998**, *38*, 209–217. [[CrossRef](#)]
5. Traore, A.; Grieu, S.; Puig, S.; Corominas, L.; Thiéry, F.; Polit, M.; Colprim, J. Fuzzy control of dissolved oxygen in a sequencing batch reactor pilot plant. *Chem. Eng. J.* **2005**, *111*, 13–19. [[CrossRef](#)]
6. Zhu, G.; Peng, Y.; Ma, B.; Wang, Y.; Yin, C. Optimization of anoxic/oxic step feeding activated sludge process with fuzzy control model for improving nitrogen removal. *Chem. Eng. J.* **2009**, *151*, 195–201. [[CrossRef](#)]
7. Holenda, B.; Domokos, E.; Redey, A.; Fazakas, J. Dissolved oxygen control of the activated sludge wastewater treatment process using model predictive control. *Comput. Chem. Eng.* **2008**, *32*, 1270–1278. [[CrossRef](#)]
8. Dominic, S.; Shardt, Y.A.; Ding, S.X.; Luo, H. An adaptive, advanced control strategy for KPI-based optimization of industrial processes. *IEEE Trans. Ind. Electron.* **2015**, *63*, 3252–3260. [[CrossRef](#)]
9. Han, H.G.; Qin, C.H.; Sun, H.Y.; Qiao, J.F. Adaptive sliding mode control for municipal wastewater treatment process. *Acta Autom. Sin.* **2023**, *49*, 1010–1018.
10. Qiao, J.F.; Han, G.; Han, H.G. Neural network on-line modeling and controlling method for multi-variable control of wastewater treatment processes. *Asian J. Control* **2014**, *16*, 1213–1223. [[CrossRef](#)]
11. Qiao, J.F.; Hou, Y.; Zhang, L.; Han, H.G. Adaptive fuzzy neural network control of wastewater treatment process with multiobjective operation. *Neurocomputing* **2018**, *275*, 383–393. [[CrossRef](#)]
12. Han, H.G.; Qiao, J.F.; Chen, Q.L. Model predictive control of dissolved oxygen concentration based on a self-organizing RBF neural network. *Control Eng. Pract.* **2012**, *20*, 465–476. [[CrossRef](#)]
13. Han, H.G.; Wu, X.L.; Qiao, J.F. Real-time model predictive control using a self-organizing neural network. *IEEE Trans. Neural Netw. Learn. Syst.* **2013**, *24*, 1425–1436. [[PubMed](#)]
14. Han, H.; Qiao, J. Nonlinear model-predictive control for industrial processes: An application to wastewater treatment process. *IEEE Trans. Ind. Electron.* **2013**, *61*, 1970–1982. [[CrossRef](#)]
15. Han, H.G.; Zhang, L.; Hou, Y.; Qiao, J.F. Nonlinear model predictive control based on a self-organizing recurrent neural network. *IEEE Trans. Neural Netw. Learn. Syst.* **2015**, *27*, 402–415. [[CrossRef](#)] [[PubMed](#)]
16. Hou, Z.S.; Wang, Z. From model-based control to data-driven control: Survey, classification and perspective. *Inf. Sci.* **2013**, *235*, 3–35. [[CrossRef](#)]
17. Hou, Z.; Jin, S. A novel data-driven control approach for a class of discrete-time nonlinear systems. *IEEE Trans. Control Syst. Technol.* **2010**, *19*, 1549–1558. [[CrossRef](#)]
18. Xu, J.; Xu, F.; Wang, Y.; Sui, Z. An Improved Model-Free Adaptive Nonlinear Control and Its Automatic Application. *Appl. Sci.* **2023**, *13*, 9145. [[CrossRef](#)]
19. Xu, D.; Jiang, B.; Liu, F. Improved data driven model free adaptive constrained control for a solid oxide fuel cell. *IET Control Theory Appl.* **2016**, *10*, 1412–1419. [[CrossRef](#)]
20. Li, J.; Tang, Z.; Luan, H.; Liu, Z.; Xu, B.; Wang, Z.; He, W. An Improved Method of Model-Free Adaptive Predictive Control: A Case of pH Neutralization in WWTP. *Processes* **2023**, *11*, 1448. [[CrossRef](#)]
21. Wang, Y.; Hou, M. Model-free adaptive integral terminal sliding mode predictive control for a class of discrete-time nonlinear systems. *ISA Trans.* **2019**, *93*, 209–217. [[CrossRef](#)]

22. Esmaeili, B.; Salim, M.; Baradarannia, M. Predefined performance-based model-free adaptive fractional-order fast terminal sliding-mode control of MIMO nonlinear systems. *ISA Trans.* **2022**, *131*, 108–123. [[CrossRef](#)]
23. Esmaeili, B.; Salim, M.; Baradarannia, M. Control of MIMO nonlinear discrete-time systems with input saturation via data-driven model-free adaptive fast terminal sliding mode controller. In Proceedings of the 2020 28th Iranian Conference on Electrical Engineering (ICEE), Tabriz, Iran, 4–6 August 2020.
24. Alex, J.; Beteau, J.F.; Copp, J.B.; Hellinga, C.; Jeppsson, U.; Marsili-Libelli, S.; Vanhooren, H. Benchmark for evaluating control strategies in wastewater treatment plants. In Proceedings of the 1999 European Control Conference (ECC), Karlsruhe, Germany, 31 August–3 September 1999.
25. Hou, Z.; Jin, S. *Model Free Adaptive Control: Theory and Applications*; CRC Press: Boca Raton, FL, USA, 2013.
26. Chiu, C.S. Derivative and integral terminal sliding mode control for a class of MIMO nonlinear systems. *Automatica* **2012**, *48*, 316–326. [[CrossRef](#)]
27. Xu, W.; Junejo, A.K.; Liu, Y.; Hussien, M.G.; Zhu, J. An efficient antidisturbance sliding-mode speed control method for PMSM drive systems. *IEEE Trans. Power Electron.* **2020**, *36*, 6879–6891. [[CrossRef](#)]
28. Xu, Q.; Li, Y. Micro-/nanopositioning using model predictive output integral discrete sliding mode control. *IEEE Trans. Ind. Electron.* **2011**, *59*, 1161–1170. [[CrossRef](#)]
29. Cao, W.; Yang, Q. Online sequential extreme learning machine based adaptive control for wastewater treatment plant. *Neurocomputing* **2020**, *408*, 169–175. [[CrossRef](#)]
30. Vilanova, R.; Katebi, M.R.; Wahab, N. N-removal on wastewater treatment plants: A process control approach. *J. Water Resour. Prot.* **2011**, *2011*, 1–11. [[CrossRef](#)]
31. Belchior, C.A.C.; Araújo, R.A.M.; Landeck, J.A.C. Dissolved oxygen control of the activated sludge wastewater treatment process using stable adaptive fuzzy control. *Comput. Chem. Eng.* **2012**, *37*, 152–162. [[CrossRef](#)]
32. Du, X.; Wang, J.; Jegatheesan, V.; Shi, G. Dissolved Oxygen Control in Activated Sludge Process Using a Neural Network-Based Adaptive PID Algorithm. *Appl. Sci.* **2018**, *8*, 261. [[CrossRef](#)]

Disclaimer/Publisher’s Note: The statements, opinions and data contained in all publications are solely those of the individual author(s) and contributor(s) and not of MDPI and/or the editor(s). MDPI and/or the editor(s) disclaim responsibility for any injury to people or property resulting from any ideas, methods, instructions or products referred to in the content.